A Platinum Open Access Journal for Organic Chemistry

Paper

Free to Authors and Readers | DOAJ Seal | *Arkivoc* **2022**, part ix, 73-89

Synthesis and anticancer activity evaluation of some new 1,2,3,5-tetrazine derivatives attached to benzothiazole moiety

Joseph Tsemeugne[a]*, Yetiny A. Bah[a], Jean P. Dzoyem[b,c], Jérôme N. Ndefongang[a], Ibukun M. Famuyide[c], Lyndy J. McGaw[c], Pamela K. Nangmo[a], Blandine M. W. Ouahouo[a], Pierre Mkounga[a], Giles Edwards[d], Peter F. W. Simon[e], Apollinaire Tsopmo[f], Emmanuel F. Sopbué[b]*, and Augustin E. Nkengfack[a]

[a]Univ. of Yaounde I, P.O. Box 812 Yaounde, Cameroon; [b]Univ. of Dschang, PO Box 67 Dschang, Cameroon; [c]Univ. of Pretoria, Private Bag X04, Onderstepoort 0110, Pretoria, South Africa; [d]The Univ. of Manchester; Oxford Road; Manchester; M13 9PL; United Kingdom; [e]Rhein-Waal Univ. of Applied Sciences, Marie-Curie Straße 1, 47533 Kleve, Germany; [f]Carleton Univ. 1125 Colonel By DriveK1S 5B6, Ottawa, Canada

Email: tsemeugne@yahoo.fr; sopbue@yahoo.fr

Received 08-28-2022 **Accepted Manuscript** 10-18-2022 **Published on line** 10-20-2022

Abstract

A series of novel tetrazine derivatives, containing benzothiazole framework, were prepared during the coupling reactions of some diazotized 2-aminobenzo[d]thiazole derivatives with p-acetaminophen. Their structures were elucidated based on NMR and MS spectrometry. The anticancer activity and the safety of the synthesized compounds along with the entire precursors were assessed against three human cancer cell lines and a normal cell line. All the synthesized compounds showed selective cytotoxic activity against the cancer cell lines used in comparison to the normal Vero cell line. Their IC50 values varied from 2.02 to 171.67 µM.

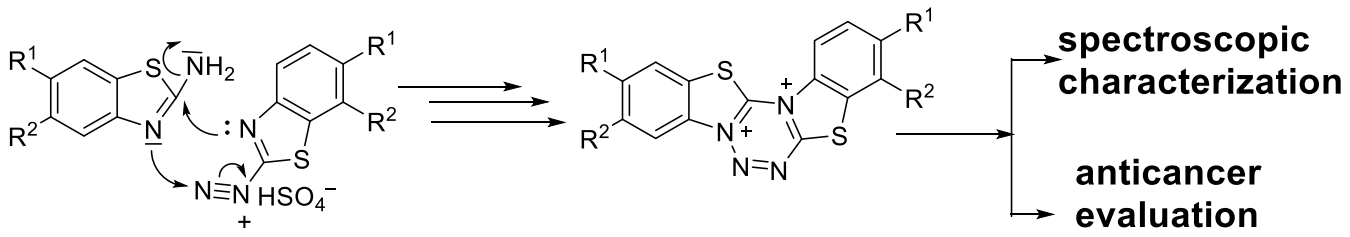

Keywords: Tetrazine, benzothiazole, acetaminophen, azo dyes, anticancer activity

Introduction

Cancer is one of the most important problems in public health and is the second leading cause of death in the world.[1] Currently, cancer chemotherapy is one of the most effective methods to treat cancer, which represents a constant, global, and interdisciplinary research effort and can heavily promote and extend the quality of life.[2] New antitumor therapies point to novel compounds with potently selective effects and must therefore exhibit a cytotoxic effect on malignant cells, without damaging normal ones. Functional materials nowadays are of particular interest in various fields that include materials science, chemistry, energy, medicine and biology.[3–5] Nitrogen-rich heterocyclic molecules particularly those of the tetrazine groups (six-membered ring with four nitrogen atoms) are used in material sciences to make high density energy compounds, because their thermal decomposition leads to the ring opening, resulting in the formation of nitriles and nitrogen molecules.[6–8] Additionally, synthetic tetrazine derivatives have been used in molecular imaging. Examples included targeted labelling, delivery of radionuclide, and visualization of tumors in lung cells and mice; fluorescent label proteins on the surface and inside mammalian cells,[9–12] and covalent bonding of tetrazine molecules to the surface of cells to study cell-to-cell interactions[13]. Synthetic tetrazine derivatives have been used in the fabrication of various architectures of polymers or hydrogels many of which are used in 3D culture printing, tissue engineering, or to preserve cell morphologies during storage.[14–18] The coupling of tetrazine to tetrazine and dienophile has been used for surface structuring and in the fabrication of microarrays.[19,20] Several tetrazine synthesis techniques are described in the literature depending on the use of the end product which can be a biological activity, diagnostics, or surface functionalization.[21-23]

There is, however, still a continuous research interest in tetrazines due to the reactivity of their unsaturated heterocyclic ring which can serve as electron donor or acceptor depending on the reaction conditions. Using tetrazine as a reactant in the search for new biologically active compounds is therefore of great importance. Thus, this work aimed to synthesize tetrazine type compounds via coupling reactions of diazonium ions of benzothiazole substrates followed by the determination of their anticancer properties in cultured cells. The process led to the synthesis of three unusual tetrazine derivatives and this might open a line of thought on the synthesis of these compounds.

Results and Discussion

Chemistry

Two 2-aminobenzothiazole derivatives were diazotized with nitrosylsulfuric acid at low temperature (0 – 5 °C). Coupling reaction was carried out by adding the diazonium solution of **1** to a solution of p-acetaminophen **3** in DMSO (Scheme 1). The chemical structures of **4** were confirmed by the available spectroscopic and elemental analysis data.

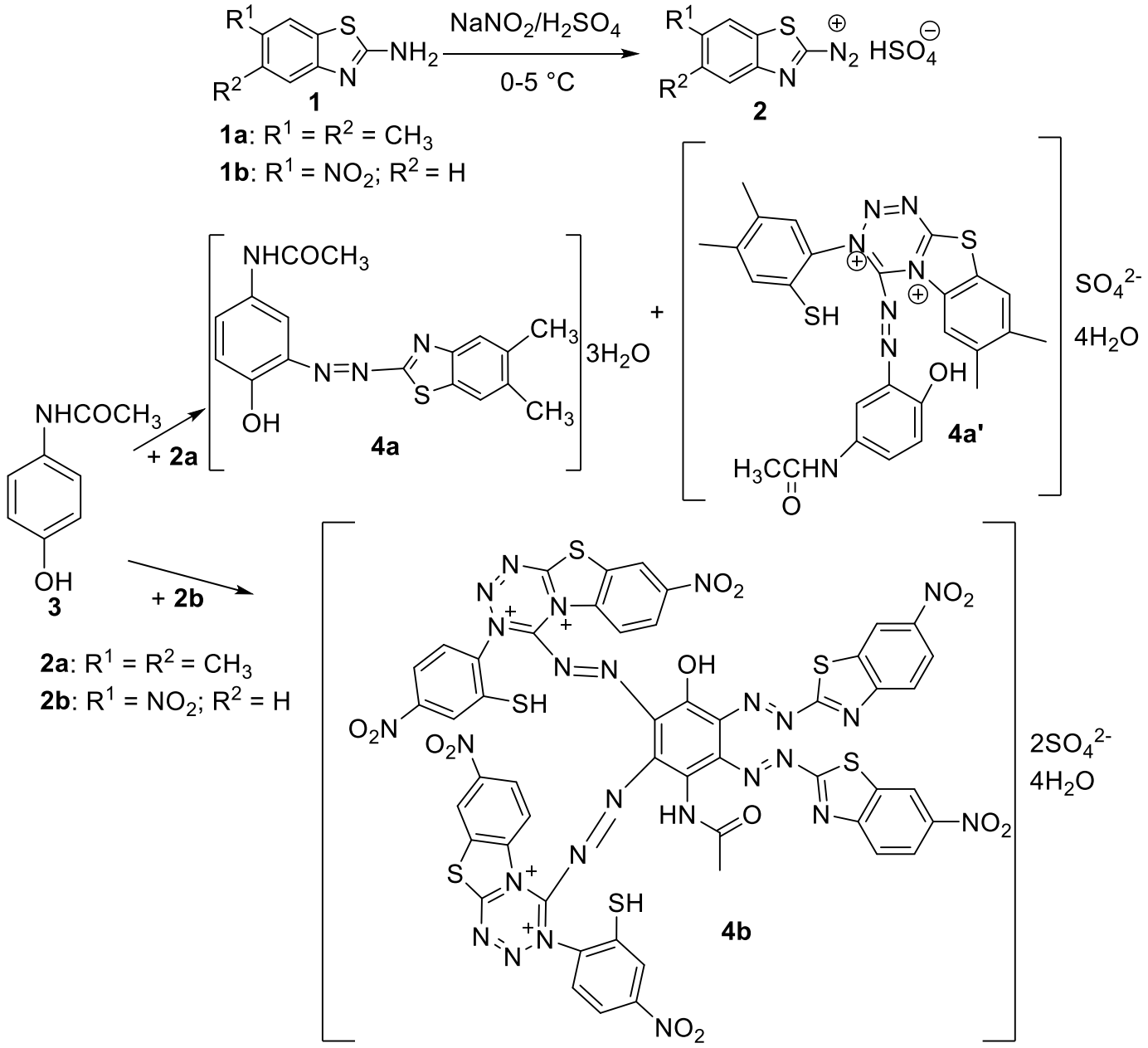

Scheme 1. Reactions' sequences to compounds **4.**

The reaction of the diazonium salt solution **2a** with **3** gave the two coupling products **4a** and **4a'** (Scheme 1). Compound **4a** was obtained as a red powder with a sharp melting point at 119 – 121 °C. The elemental analysis and the High Resolution Electron Impact Mass Spectroscopy-experiments were used to establish the gross formula as $C_{17}H_{22}N_4O_5S$ showing that the coupling product crystallized with three molecules of H_2O. The HRMS showed the molecular ion peak at *m/z* 395 corresponding to ($M^{+\cdot}$ + H). Characteristic ion fragments were rationalized from the spectrum at *m/z* = 338 ($M^{+\cdot}$ + H – N_2 – $2CH_3$), 332 ($M^{+\cdot}$ + H – H_2O – $3CH_3$), 310 (M^{+}– $3H_2O$ – $2CH_3$), 284 ($M^{+\cdot}$ + H – $NCOCH_3$– $3H_2O$). These results were confirmed by the IR-experiment which exhibited a large band in the higher frequency region around 3248 cm^{-1} due to the combined stretching frequencies of the phenolic-OH and the hydroxyl groups of H_2O. The stretching frequencies of the aromatic C-H appeared at 2922 cm^{-1}, whereas the combined stretching frequencies of the carbonyl groups could be observed as an intense

band around 1659 cm^{-1}. The characteristic stretching frequencies of the diazo bridges were exhibited between 1450 and 1483 cm^{-1}.

Table 1. Comparison of ^{1}H- and ^{13}C (^{1}H)-NMR data of **4a** with the simulated values

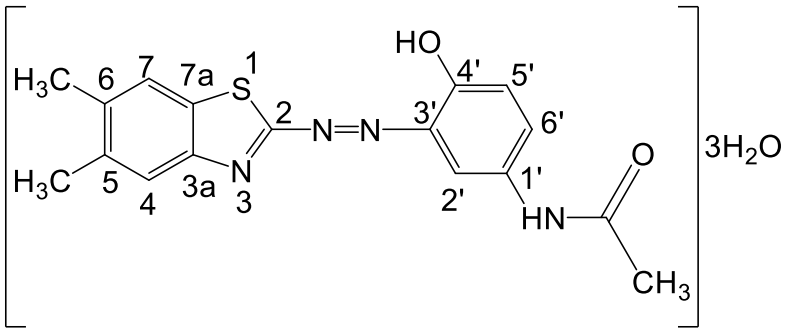

	δ_H in ppm (multiplicity, J in Hz)		δ_C in ppm	
N° (H, C)	Simulated values	Experimental values	Simulated values	Experimental values
2			169.8	168.1
3a			151.6	153.6
4	7.27 (d, J = 0.49)	7.89 (s, 1H)	119.0	122.5
5			130.9	132.1
6			133.9	137.4
7	7.28 (d, J = 0.49)	7.84 (s, 1H)	121.3	124.2
7a			130.1	131.3
1'			137.5	138.5
2'	7.39 (dd, J = 2.49 and 0.50 Hz)	8.10 (d, J = 2.0 Hz, 1H)	115.0	108.1
3'			132.1	136.1
4'			149.5	151.1
5'	6.79 (dd, J = 8.66 and 0.50 Hz)	7.06 (d, J = 8.0 Hz, 1H)	115.9	118.8
6'	7.05 (dd, J = 8.66 and 2.49 Hz)	7.60 (dd, J = 8.0 and 2.0 Hz, 1H)	120.5	128.1
CO			168.7	174.6
$COCH_3$	2.07 (s)	2.01 (s, 3H)	23.2	23.8
CH_3	2.32 (s)	2.36 (s, 3H)	20.0	19.9
CH_3	2.34 (s)	2.36 (s, 3H)	20.0	19.6

On the ^{1}H-NMR spectrum, the benzothiazole protons H-4 and H-7 resonated at δ_H = 7.89 and 7.84 ppm as a singlet, while the singlets observed at δ_H = 10.63 and 9.94 ppm were respectively assigned to the OH-group and NH proton of the acetaminophen. Dye **4a** showed a singlet peak at 2.36 ppm for methyl groups fixed on benzothiazole ring and a peak at 2.01 ppm for $COCH_3$ protons on the acetaminophen ring. Besides, one poorly

resolved "dd"-signals [centered at 7.60 ppm (H-6', J = 2.00 and 8.00 Hz) and a set of two couples of poorly resolved "d"-signals [centered at 8.10 ppm (H-2', J = 2.00 Hz) and 7.06 ppm (H-5', J = 8.00 Hz) overlapping in the range 7.06 - 8.10 ppm, were attributed to the ABX proton systems in the acetaminophen unit of the coupling product.

The ^{13}C-NMR-spectrum exhibited 17 relevant signals, out of which eight could be assigned to the methyl carbon and the aromatic tertiary C-H carbons, and nine to the quaternary carbon atoms. The assignment of ^{1}H- and ^{13}C (^{1}H)-NMR data for compound **4a** was done by comparison with simulated values (table 1).

In the coupling reaction of **2a** with **3**, it was observed that the anticipated compound **4a** is first formed and a part of it subsequently undergoes *in situ* nucleophilic addition with another part of unreacted **2a** to yield tetrazine **4a'** (Scheme 2). A plausible mechanism for the reaction may consist in the first step of the nucleophilic attack of the diazo function of diazonium salt **2a** by the heteroaromatic nitrogen atom of the azobenzothiazole **4a** as shown in Scheme 2. In the second step, the heteroaromatic N atom of the newly introduced benzothiazole fragment operates an intramolecular nucleophilic attack on the highly electron deficient sp^2 C of the other thiazole ring to form the unstable fused five ring intermediate system incorporating the tetrazine unit. The latter subsequently rearranges with proton abstraction from the hydrogen sulfate ion (HSO_4^-), resulting into the opening of the thiazole ring of the first benzothiazole moiety with the formation of the thiol function. This hypothesis is in agreement with recent reports[24,25] mentioning the high reactivity of the heteroaromatic N atom of benzothiazole under similar reactions conditions.

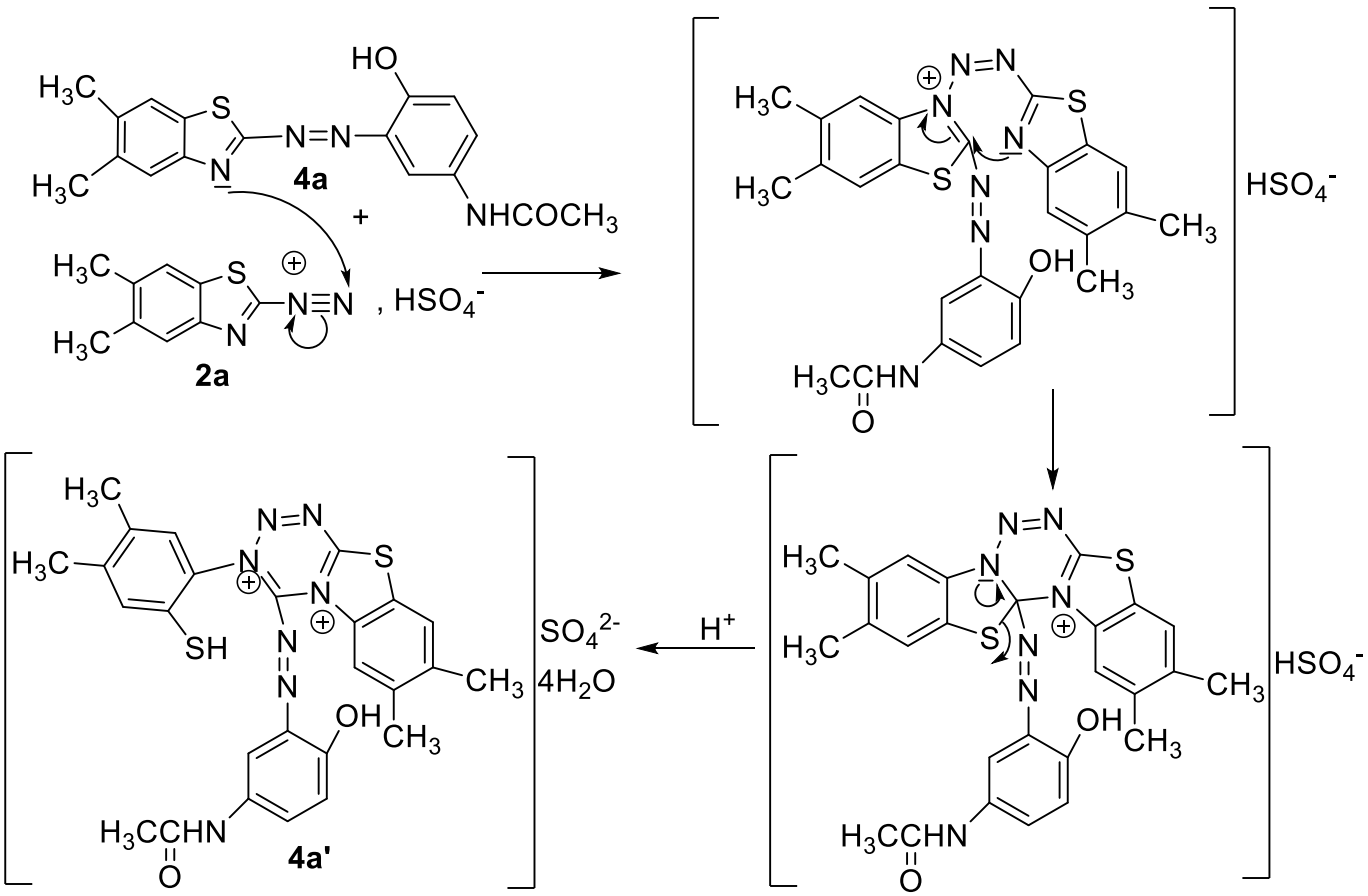

Scheme 2. The plausible mechanism for the synthesis of **4a'.**

The structure of compound **4a'** has been elucidated by various spectroscopic techniques such as ^{1}H-NMR and ^{13}C-NMR spectra and elemental analysis.

Compound **4a'** was obtained as a brown powder with a sharp melting point in the range of 318 – 320 °C. The elemental analysis and the HREIMS-experiments were used to establish the gross formula as $C_{26}H_{33}N_7O_{10}S_3$ showing that the coupling product crystallized with one sulfate ion SO_4^{2-} and four molecules of H_2O. Further supporting evidences were obtained from the elemental analysis and the HREIMS, which confirmed the molecular mass to be 699, with relevant ion-fragments at *m/z* = 673 ($M^{+\cdot}$– CN), 643 ($M^{+\cdot}$– $2N_2$), 601 ($M^{+\cdot}$– H_2SO_4), 599 ($M^{+\cdot}$– H_2SO_4 – H_2), 581 ($M^{+\cdot}$– CH_3CONH – N_2 – S). The ion fragment at *m/z*: 563 ($M^{+\cdot}$ – C_8H_8S), 385 ($M^{+\cdot}$ – C_8H_8S – $C_8H_8N_3O_2$) and 283 ($M^{+\cdot}$ – C_8H_8S – $C_8H_8N_3O_2$ – C_8H_8) were assigned as in scheme 3, confirming the above structural hypothesis.

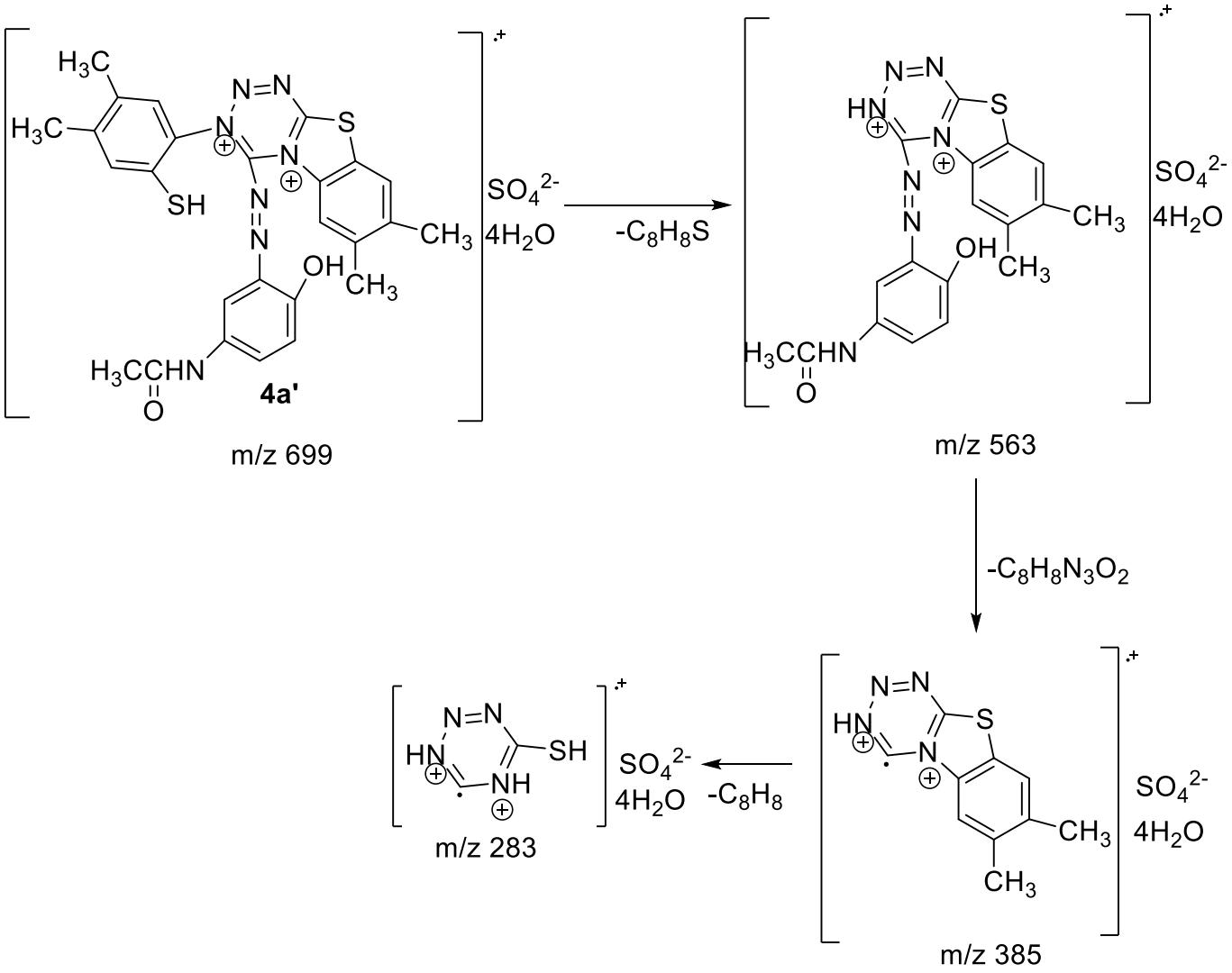

Scheme 3. HRMS fragmentation patterns of compound **4a'.**

These results were also confirmed by the IR-experiment which exhibited a large band in the higher frequency region around 3887-3284 cm^{-1} due to the combined stretching frequencies of the phenolic-OH and the hydroxyl groups of H_2O. The stretching frequencies of the aromatic C-H appeared at 2920 cm^{-1} while those of S-H appeared at 2324 cm^{-1}. Two additional bands due to the tetrazine group[26] appear at 1370 and 889 cm^{-1}.

The structure of synthetic tetrazine was determined based on the ^{1}H and ^{13}C NMR chemical shifts and on the proton-proton coupling constants. On the ^{1}H-NMR spectrum, the protons of the methyl on benzothiazole ring resonated at δ_H = 2.50, 2.39, 2.37, and 1.23 ppm respectively as singlets, while the singlet observed at δ_H = 2.04 ppm was assigned to the methylketone protons.[27] In the phenolic moiety, we have an ABX Proton system at 8.13 (d, 1H, J = 2.8 Hz, H-6'), 7.63 (dd, 1H, J = 8.8 and 2.8 Hz, H-4') and 7.09 (d, 1H, J = 8.8 Hz, H-3') confirming the proposed regio-orientation of the electrophilic substitution of the benzothiazole diazonium ion at the ortho-position to the OH-group in the acetaminophen reagent.

The ^{1}H-NMR spectrum showed seven sets of aromatic Csp2-H protons at 8.37 (s, 1H, H-9'''), 8.13 (d, 1H, J = 2.8 Hz, H-6'), 7.93 (s, 1H, H-6'''), 7.77 (s, 1H, H-6''), 7.69 (s, 1H, H-3''), 7.63 (dd, 1H, J = 8.8 and 2.8 Hz, H-4') and 7.09 (d, 1H, J = 8.8 Hz, H-3').

The ^{13}C-NMR spectrum of the tetrazine shows 24 signals attributable to 26 carbon atoms. In addition, the characteristic signals of five methyl groups (CH_3) appearing at δ = 23.82 ppm, 23.78 ppm, 19.86 ppm, 19.67 ppm and 19.61 ppm, are in agreement with the presence of two benzothiazoles units in the assigned structure of **4a'**. A remarkable feature in the ^{13}C-NMR spectrum of this compound is the intense downfield shifts (Δδ = 30.5 ppm) of the δ_C of the carbon 4 of the tetrazine rings add to diazo function respectively from 168.14 ppm in the benzothiazole substrate[27] **4a** to 198.6 ppm in the tetrazine product.

The UV spectrum of the tetrazine exhibits absorptions between 270 and 640 nm, in the visible range. Table 2 below recapitulates some characteristics wavelengths maxima and the corresponding molar extinction coefficients. A comparison of the UV spectrum of the tetrazine with that of the starting azo dye allows us to observe a weak bathochromic effect and the appearance of new bands on the spectrum of the tetrazine, in agreement with the extension of the chromophore system resulting from the condensation reaction.

Table 2. UV-vis data of **4a** and **4a'**

	λ (nm)	ε ($L.mol^{-1}.cm^{-1}$)
Compound **4a**	274	100000
	327	24900
	364	30600
	452	10400
Compound **4a'**	301	60400
	339	51300
	369	51500
	565	13800
	644	13900
	746	3500

The above assumption that the involvement of the heteroaromatic N of the benzothiazole in the inter- and intramolecular nucleophilic attack respectively in the first and second step of the reaction's mechanism of scheme 2 is due to the lack of suitable electrophilic positions on the aromatic ring of the benzothiazole used as coupler, prompted us to investigate the behavior of the diazonium salt **2b** in the presence of **1b** (Scheme 4). As anticipated, tetrazine **4c** and the coupling product of two equivalents of **2b** molecules **4c'** formed as previously described[27] were isolated from this reaction.

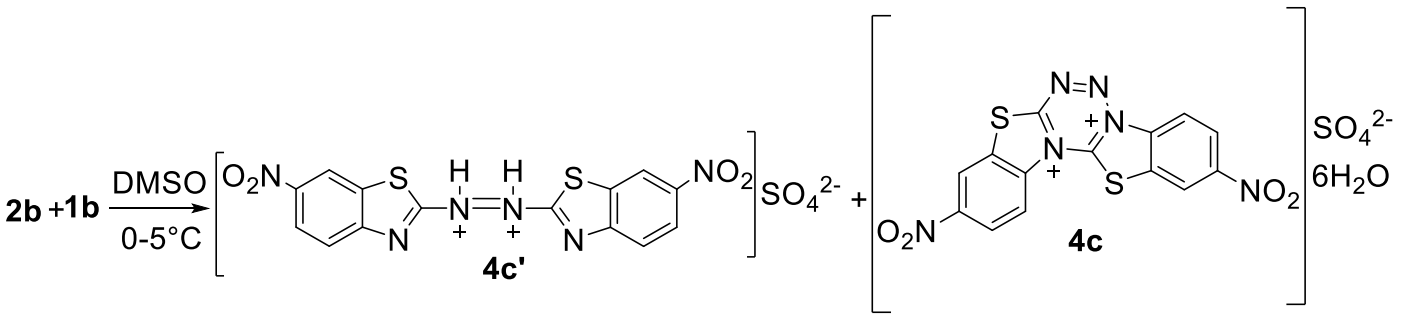

Scheme 4. Reaction's sequence to compounds **4c** and **4c'.**

The formation of compound **4c** certainly results from the subsequent nucleophilic addition of the heteroaromatic nitrogen atom of the benzothiazole ring (Scheme 5).

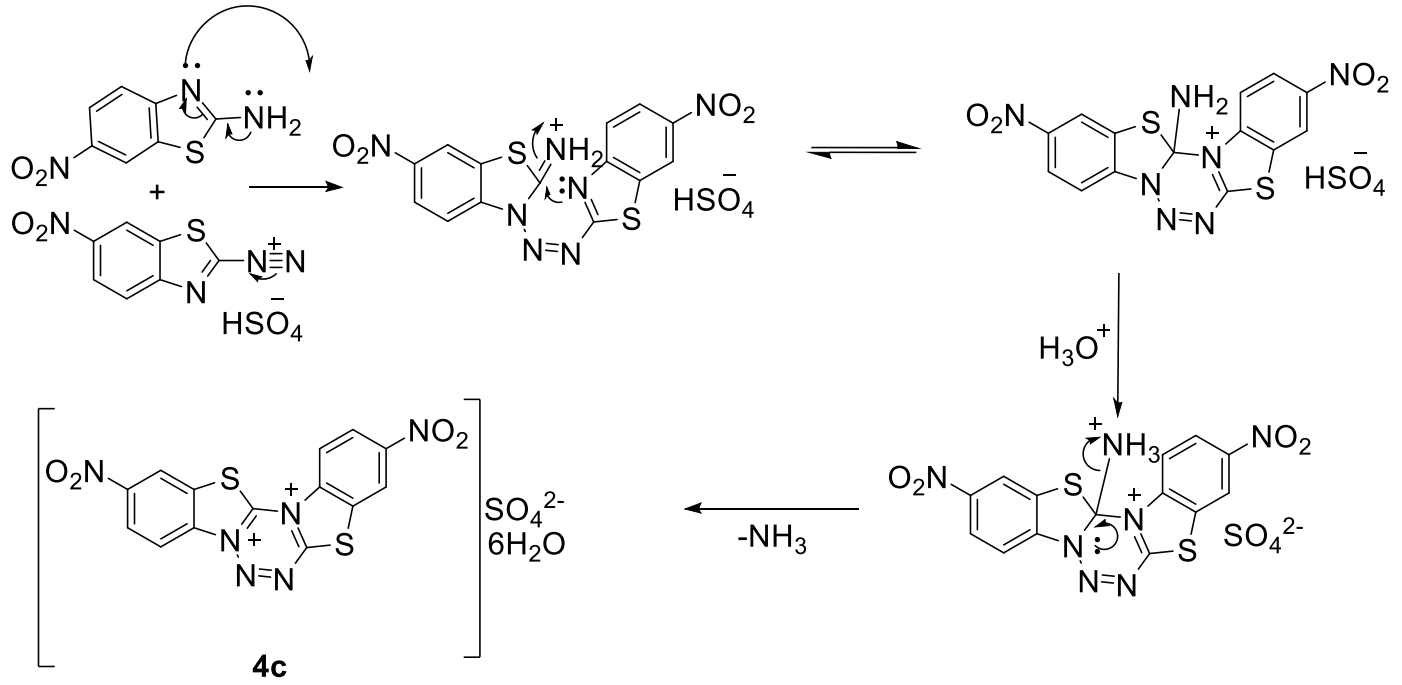

Scheme 5. The plausible mechanism for the formation of compound **4c.**

Based on the structure of 1,2,3,5-tetrazine, this molecule not only has π* orbitals, but also nonbonding n orbitals. So, these orbitals contribute to two kinds of transition: n→π* transition and π→π* transition. The absorption spectra of tetrazine **4c**, shows two main absorption bands: one around 260 nm corresponding to the π→π* transition analogue to benzene and a second is around 450 nm due to the n→π* transition. According to Mason, the broad absorption band appearing around 352 nm in solutions is due to an additional n→π* transition.[28] Similar observations were reported earlier.[29]

Compound **4c** was obtained as an orange powder with a melting point in the range of 245 – 247 °C. The elemental analysis and the electrospray mass spectra-experiments were used to establish the gross formula as $C_{14}H_{18}N_6O_{14}S_3$ showing that the coupling product crystallized with one sulfate ion, and six molecules of H_2O. The electrospray mass spectrum showed the molecular ion peak at *m/z* 590 corresponding to $[M]^{+\cdot}$. Surface ligand exchange behaviours of compounds **4c** by primary alcohols using electrospray ionization mass

spectrometry (ESI-MS) were clearly established.[27] Methanol was used as a model primary alcohol for the analysis. As clearly proven by peaks at *m/z* = 568, the surface of tetrazine **4c** is partly exchanged by methanol within 1 min to give peaks ($M^{+\cdot} - 3H_2O + MeOH$). The ion-fragments at *m/z* = 513 ($M^{+\cdot} - 3H_2O + MeOH - 2H_2O$), 450 ($M^{+\cdot} - 3H_2O + MeOH - H_2 - H_2SO_4$), 378 ($M^{+\cdot} - 3H_2O + MeOH - C_6$), 294 ($M^{+\cdot} - 3H_2O + MeOH - C_4H_2 - 2HO^-$) and 247 ($M^{+\cdot} - 3H_2O + MeOH - NO_2$), were assigned as in scheme 6, confirming the above hypothesis (Scheme 6).

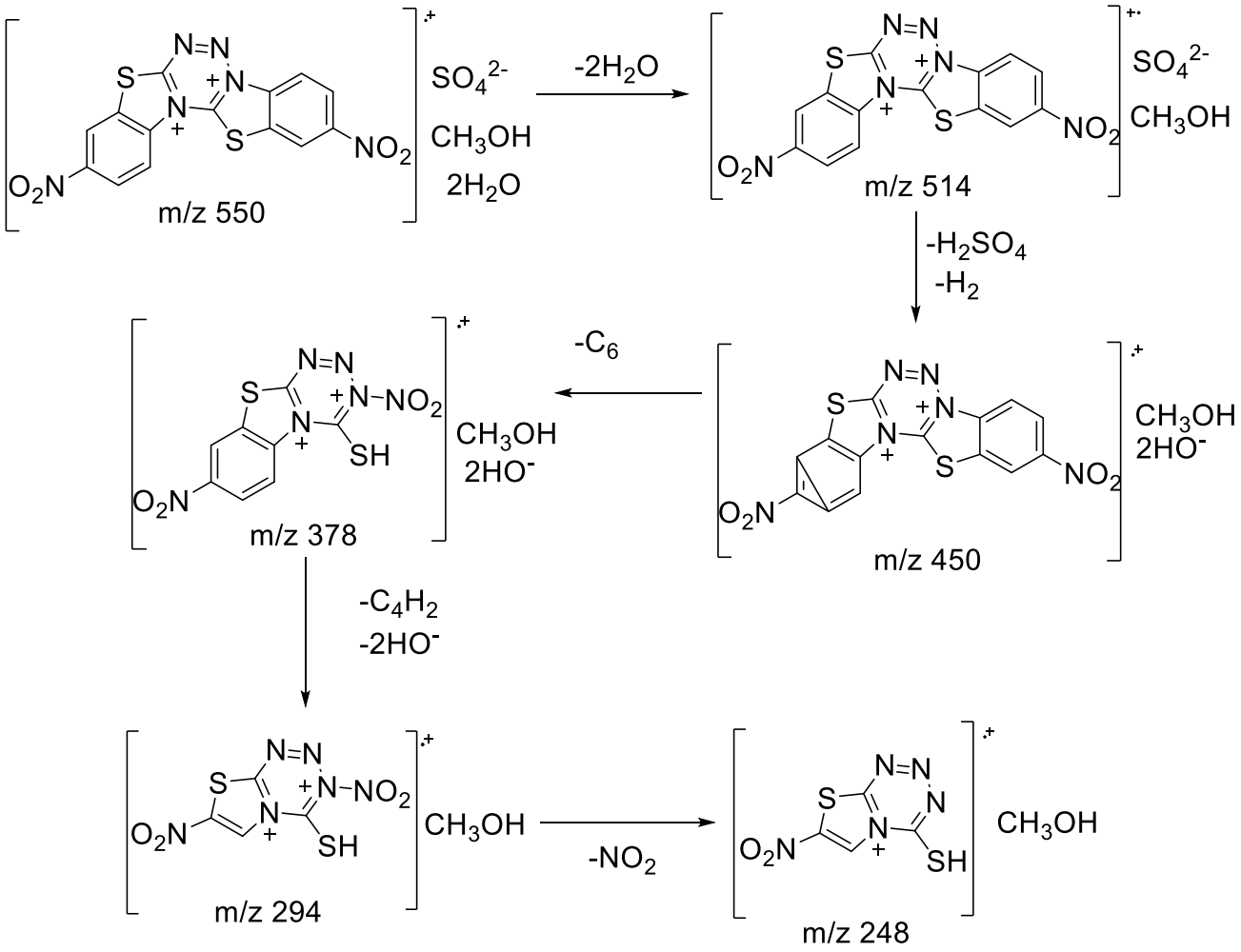

Scheme 6. HRMS fragmentation patterns of compound **4c** highlighting surface ligand exchange behaviours by MeOH.

The FTIR spectrum of compound **4c** shows typical absorption bands due to aromatic C-H-stretching vibrations at 3097 cm^{-1}, aromatic C=C-stretching and ring deformation vibrations at 1514 and 718 cm^{-1} respectively. Two additional bands due to the tetrazine moiety appear at 1336 and 908 cm^{-1}.[29]

The ^{1}H-NMR spectrum of compound **4c** gave signals at δ_H [7.90 (d, 1H, J = 8.8 Hz, H-4), 8.25 (dd, 1H, J = 2.8 and 8.8 Hz, H-5), 8.95 (d, 1H, J = 1.8 Hz, H-7)] and [7.42 (d, 1H, J = 8.8 Hz, H-4'), 8.11 (dd, 1H, J = 2.4 and 8.8 Hz, H-5'), 8.69 (d, 1H, J = 2.4 Hz, H-7'), attributable to two ABX systems of nitrobenzothiazole, confirming the proposed regio-orientation of the nucleophilic addition of the heteroaromatic N of the benzothiazole **1b** with diazonium ion **2b** instead of electrophilic substitution to yields compounds **4C** and/or **4C'** (figure 1) as anticipated.

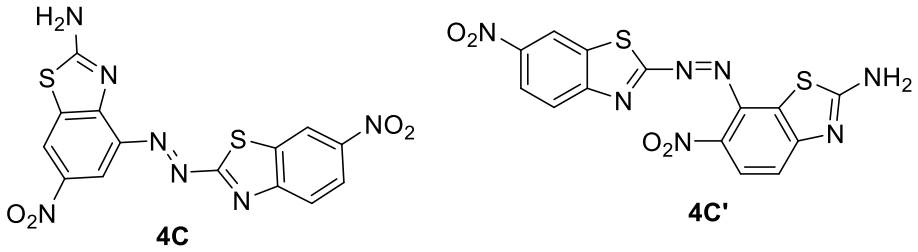

Figure 1. most plausible alternative structures for compound **4c.**

The ^{13}C-NMR spectrum of compound **4c** exhibited 13 carbon signals instead of 14 as required by the molecular formula. This could be explained by the overlapping of the signals of carbon C-5 and C-5' at δ_C 122.5 ppm due to their magnetic and chemical equivalence. The analysis made on the HSQC spectrum of compound **4c** shows six correlation spots which confirm the presence of six methines (=C-H) in its structure. This spectrum also allows us to clearly establish that, although carbons C-5 and C-5' have the same chemical shift, they correlate with two distinct protons at δ_H 8.25 and δ_H 8.11 ppm respectively, proving that the signal at δ_C 122.5 ppm corresponds to two carbons.

The structure of compounds **4b** and **4c'** were assigned based on their analytical and spectral data following similar reasonings as above.

Anticancer activity

The anticancer activity and the safety of the synthesized compounds along with the entire precursors were assessed against three human cancer cell lines (A549, Hela and MCF-7) and a normal cell line (Vero cells). Doxorubicin was used as a reference control drug. Their median inhibitory concentrations (IC_{50}) are presented in Table 3.

Table 3. Cytotoxicity of synthesized compounds and reference anticancer drugs

Compounds	IC_{50} (µM)				Selectivity index		
	Vero	A549	Hela	MCF-7	A549	Hela	MC7
1a	>200	74.52±6.80	171.67±8.7	91.1±9.2	>2.68	>1.17	>2.20
1b	104.18±7.59	98.72±6.61	71.54±5.18	89.74±4.86	1.06	1.46	1.16
3	>200	>200	>200	>200	nd	nd	nd
4a	94.53±1.87	26.79±2.89	17.91±2.80	20.44±2.11	3.53	5.28	4.62
4a'	28.82±2.17	**5.31±1.33**	14.54±1.29	16.47±1.03	5.43	1.98	1.75
4b	14.65±1.54	**2.02±2.14**	**2.05±2.55**	13.65±1.44	7.15	7.25	1.07
4c	27.26±1.31	**6.48±0.72**	**8.22±2.44**	18.66±1.54	4.21	3.32	1.46
4c'	57.72±3.98	55.19±3.62	65.17±3.31	49.19±2.36	1.05	0.89	1.17
Doxorubicin	**1.67±0.72**	**0.88±0.35**	**0.33±0.45**	**1.05±0.86**	1.87	5.06	2.54

Nd: Not determined. In bold are values of significant activity[30]

Benzothiazole possesses wide spectrum biological activities including anti-inflammatory, antibacterial, antioxidant, antiviral, anti-tumour, anticancer and anti-proliferative, among others.[31] In addition, tetrazine and benzothiazole derivatives have been an attractive subject due to their potential anticancer activity in medicinal chemistry.[32] Therefore, all the synthesized compounds were tested for their cancer cell proliferation inhibiting activity. Results showed selective cytotoxicity against the cancer cell lines tested compared to the

normal Vero cell line. Their IC_{50} values varied from 2.02 µM to 171.67 µM. Compared to their precursors, all the synthesized compounds had increased inhibition of the three human cancer cells. Interestingly, none of the tested compounds had any significant cytotoxicity against non-cancerous Vero cells. Among the tested compounds, compound **4b,** a tetrazine derivative, had the most potent inhibitory activity on the three cancer cell lines (A549, Hela and MCF-7) with IC_{50} values of 2.02 µM, 2.059 µM, and 13.65 µM, respectively. The activity of compound **4b** against A549 and Hela cells was close to that of the standard cytotoxic anticancer drug doxorubicin (IC_{50} values of 0.88 µM and 0.33 µM respectively). According to recommended *in vitro* cytotoxic activity cutoff values a compound is considered to be cytotoxic if the IC_{50} < 10 µM.[33] Based on this recommended value, the cytotoxicity of compounds **4a**, **4a'** and **4b** can be considered significant. This finding is in agreement with relevant literature since several compounds containing the 1,2,4,5-tetrazine skeleton have been synthesized and evaluated for their antitumor activities and these compounds have been shown to exhibit potent antiproliferative activities against a panel of cancer cells including MCF-7.[34,35] Although the two 2-aminobenzothiazole compounds **1a** and **1b** used as starting materials in this study showed moderate anticancer activity, several reports have documented benzothiazole derivatives as anticancer agents.[31]

Specific killing of cancer cells without affecting healthy cells is a key safety feature of any cancer chemotherapy; therefore, the selectivity index for cancer cell lines A549, Hela and MCF-7 was calculated from the ratio of their respective IC_{50} values and that of Vero normal cells (Table 3). The SI values of the tested compounds ranged from 0.89 to 7.15. As the SI value highlights the differential activity of a compound, the greater the SI value the more selective is the compound. The SI significance of compounds has been classified as follow: SI ≤ 1 = no selectivity, 1 < SI < 5 = moderate selectivity, SI ≥ 5 = strong selectivity.[30] Considering these criteria, it can be deduced that compounds with good anticancer activity also displayed strong selectivity index values in terms of activity against Vero cells. SI values less than 1 indicate the general toxicity of the pure compound.

Conclusions

Herein, a straightforward synthetic approach for the preparation of 1,2,3,5-tetrazine with benzothiazole moieties as pendant groups was introduced. The new 1,2,3,5-tetrazines containing benzothiazole backbones were successfully synthesized at a temperature of 0–5 °C and fully characterized by available elemental and spectroscopic data. Compound **4b** exhibited potent activity against A459 and Hela cells, with strong selectivity calculated in terms of activity against non-cancerous Vero cells. These findings could be helpful for the design and synthesis of lead compounds with the structural scaffold of 1,2,3,5-tetrazine for the development of new anticancer therapeutic agents. Future studies will involve the determination of the mechanism of anticancer activity of these compounds.

Experimental Section

Chemistry

General. Melting points were determined on a Buchii melting point apparatus and are uncorrected. The Thin Layer Chromatography (T.L.Cs) was carried out on Eastman Chromatogram Silica Gel Sheets (13181; 6060) with fluorescent indicators. A mixture of hexane and ethyl acetate (4:6) was used as the eluent and iodine was used for the visualization of the chromatograms. The IR spectra were measured with a Fourier Transform

Infrared spectrometer JASCO FT/IR-4100 and a Perkin Elmer FT-IR 2000 spectrometer. The UV spectra were recorded with a Beckman U-640 Spectrophotometer, using samples' solutions of concentration 5×10^{-5} mol.L^{-1}. Combustion analyses were carried out with a Euro EA CHNSO analyser from Hekatech company, and the results were found to be in good agreement (±0.3%) with the calculated values. Positive ion electrospray mass spectra were recorded on a Waters Xevo TQD tandem quadrupole mass spectrometry system running in MS scan mode, 1 minute of acquired spectra were combined and centroided. ^{1}H-NMR spectra were recorded in DMSO-d_6 with a 400 MHz spectrometer NMR Bruker Advance 400. ^{13}C-NMR spectra were recorded in DMSO-d_6 with a 100 MHz spectrometer NMR Bruker Advance 400. Tetramethylsilane (TMS) was used as the internal reference. Simulated ^{1}H- and ^{13}C(^{1}H)-NMR-spectra were performed using http://www.nmrdb.org/ spectral simulation software.

Preparation of the reagents and starting materials. All the reagents mentioned in this work were purchased from Aldrich and Fluka and were used without further purification.

Preparation of diazonium salt solution. In a similar manner as earlier described[27], dried sodium nitrite (0.69 g, 10 mmol) was slowly added over a period of 30 minutes to concentrated sulphuric acid (10 mL) with occasional stirring. The solution was cooled to 0-5 °C. Compound **1** was dissolved in DMSO (10 mL) and cooled to 0–5 °C. The nitrosyl sulphuric acid solution was added to the solution of **1** and the temperature was maintained between 0–5 °C. The clear diazonium salt solution thus obtained consisting of the *in situ*-formed intermediate **2**, was used immediately in the coupling reactions.

General procedure for the preparation of the coupling products 4. Acetaminophen (**3**) (1.51 g, 10 mmol) or 2-amino-6-nitrobenzothiazole (**1b**) (1.952 g, 10 mmol) was dissolved in DMSO (10 mL) and then cooled in an ice-bath at 0–5 °C. The previously prepared diazonium solution of **2** was added drop wise over 1 hour, and then 15 mL of sodium acetate solution (10%) was added to the mixture. The pH of the mixtures was in the range 9–11. The solid precipitate was collected on a filter and crystallised from methanol to give the title compound.

***N*-(3-((5,6-Dimethylbenzo[d]thiazol-2-yl)diazenyl)-4-hydroxyphenyl)acetamide (4a).** Compound **4a** was obtained in 58% yield as red powder; m.p. 119 – 121 °C; ^{1}H-NMR (DMSO-d_6, 400MHz): δ 10.67 (s, 1H, O-H), 9.94 (s, 1H, N-H), 8.10 (d, 1H, *J* 4.0 Hz, H-2'), 7.89 (s, 1H, H-4), 7.84 (s, 1H, H-7), 7.60 (dd, 1H, *J* 4.0 and 8.0 Hz, H-6'), 7.06 (d, 1H, *J* 8.0 Hz H-5'), 2.36 (s, 6H, 2CH_3), 2.01 (s, 3H, $COCH_3$); ^{13}C-NMR (DMSO-d_6,100 MHz): δ 174.6 (CO), 168.1 (C-2), 153.6 (C-3a), 131.3 (C-4a), 124.2 (C-4), 137.4 (C-5), 132.1 (C-6), 122.5 (C-7), 138.5 (C-1'), 108.1 (C-2'), 136.1 (C-3'), 151.1 (C-4'), 118.8 (C-5'), 128.1 (C-6'), 23.8 (CH_3CO), 19.9 (CH_3), 19.6 (CH_3); UV-Vis λ_{max} (DMSO) (Log ε): 274 (5.00), 327 (4.39), 364 (4.49), 452 (4.01) nm; IR (KBr) υ_{max}: 3248 (O-H and N-H), 1659 (C=O), 1604-1557 (C=C), 1483-1450 (N=N), 1274 (C-S), 1239 (C-S), 861-510 (Ar def C=N str thiazole) cm^{-1}. (ESI^{+}) *m/z* (%) 394 (8), 389 (10), 375 (13), 372 (7), 316 (65), 304 (48), 283 (19), 202 (14), 192 (21), 150 (70); Anal. Calcd. for $C_{17}H_{22}N_4O_5S$: C, 59.98; H, 4.74; N, 16.46; S, 9.42. Found: C, 59.63; H, 4.80; N, 16.41; S, 9.40. Rf = 0.62.

4-((5-Acetamido-2-hydroxyphenyl)diazenyl)-3-(2-mercapto-4,5-dimethylphenyl)-7,8-dimethylbenzo[4,5]thiazolo[2,3-d][1,2,3,5]tetrazine-3,5-diium sulfate (4a'). Compound **4a'** was obtained in 34% yield as brown powder; m.p. 318 – 320 °C; ^{1}H-NMR (DMSO-d_6, 400 MHz): δ 11.35 (s, 1H, OH), 10.67 (s, 1H, NH), 8.37 (s, 1H, H-9'''), 8.13 (d, 1H, *J* 2.8 Hz, H-6'), 7.93 (s, 1H, H-6'''), 7.77 (s, 1H, H-6''), 7.69 (s, 1H, H-3''), 7.63 (dd, 1H, *J* 8.8 and 2.8 Hz, H-4'), 7.09 (d, 1H, *J* 8.8 Hz , H-3'), 2.50 (s, 3H, CH_3), 2.39 (s, 3H, CH_3), 2.37 (s, 3H, CH_3), 1.23 (s, 3H, CH_3), 2.04 (s, 3H, $COCH_3$); ^{13}C-NMR (DMSO-d_6, 100 MHz): δ 198.6 (C-4), 174.5 (C=O), 168.1 (C-6), 153.5 (C-1''), 151.0 (C-2'), 138.4 (C-5'''), 137.4 (C-8''' and C-5'), 136.0 (C-5''), 132.1 (C-7'''), 131.3 (C-4''' and C-2''), 128.1 (C-1'), 124.2 (C-4''), 122.4 (C-3''), 122.1 (C-9'''), 121.6 (C-6'''), 118.8 (C-6''), 118.3 (C-4'), 108.0 (C-3'), 105.4 (C-6'), 23.8 ($CO\underline{CH_3}$), 23.7 (Ph-CH_3), 19.86 (Ph-CH_3) , 19.7 (Ph-CH_3), 19.6 (Ph-CH_3); UV-Vis λ_{max} (MeOH) (Log ε): 227 (4.06), 257 (4.12), 272 (4.26), 290 (4.09), 295 (4.08), 302 (4.12), 325 (4.19), 348 (4.18), 355 (4.19),

399 (4.23), 445 (4.25), 486 (4.22) nm; IR (KBr) ν_{max} : 3887-3282 (O-H and N-H), 2920 (ArC-H), 2324 (S-H), 1664-1655 (C=O), 1533 (C=C), 1490-1449 (N=N), 1370 ($\delta_{tetrazine\ ring}$), 1269 (C-S), 1240 (C-O), 889 ($\delta_{tetrazine\ ring}$) cm^{-1}; ms: (ESI^+) *m/z* (%) 699 (8), 673 (9), 643 (11), 659 (75), 601 (10), 599 (58), 581 (22), 485 (41), 410 (34), 409 (74), 316 (100), 166 (47); Anal. Calcd. for $C_{26}H_{33}N_7O_{10}S_3$: C, 44.63; H, 4.75; N, 14.01; S, 13.74. Found: C, 44.59; H, 4.80; N, 14.05; S, 13.71. Rf = 0.30.

***N*-4-Hydroxy-2,3-bis[3-(3-nitro-benzenethiol-5)-yl-7-nitro-9-thia-1,2-diaza-3,4a-diazonia-fluorene-4)-yl-diazenyl]-5,6-bis[(6-nitro-benzothiazol-2)-yl-diazenyl]-phenyl-acetamide disulfate** (**4b**). Compound **4b** was obtained in 67% yield as brown powder; m.p. 171 – 173 °C; ^{1}H-NMR (DMSO-d_6, 400 MHz): δ 8.65 (d, 1H, *J* 2.4 Hz, H-8^v), 8.58 (d, 1H, *J* 2.8 Hz, H-4'), 8.43 (dd, 1H, *J* 8.8 and 2.8 Hz , H-5'), 8.43 (dd, 1H, *J* 9.2 and 2.4 Hz, H-6^v), 8.38 (dd, 1H, *J* 8.8 and 2.4 Hz, H-4^{iv}), 8.38 (dd, 1H, *J* 9.2 and 2.0 Hz, H-6^{vii}), 8.31 (d, 1H, *J* 9.2 Hz, H-5^v), 8.20 (dd, 1H, *J* 6.4 and 2.0 Hz, H-4^{viii}), 8.19 (d, 1H, *J* 2.4 Hz, H-2^{iv}), 8.18 (d, 1H, *J* 6.4 Hz, H-2^{viii}), 8.10 (dd, 1H, *J* 8.8 and 2.4 Hz, H-5''), 7.85 (d, 1H, *J* 8.8 Hz, H-4''), 7.68 (d, 1H, *J* 2.0 Hz, H-5^{viii}), 7.42 (d, 1H, *J* 9.2 Hz, H-8^{vii}), 7.35 (d, 1H, *J* 2.0 Hz, H-5^{vii}), 7.28 (d, 1H, *J* 8.8 Hz, H-7'), 7.13 (d, 1H, *J* 2.4 Hz , H-7''), 7.05 (d, 1H, *J* 8.8 Hz, H-5^{iv}), 3.17 (s, 2H, SH), 2.05 (s, 3H, $COCH_3$); ^{13}C-NMR (DMSO-d_6, 100 MHz): δ 180.4 (CO), 171.7 (C-4'''), 170.5 (C-4^{vi}), 169.8 (C-2'), 168.3 (C-2''), 168.0 (C-4), 158.2 (C-3^{vii}), 155.8 (C-3a'), 155.3 (C-3a''), 155.1 (C-3^{iv}), 152.5 (C-7^v), 145.3 (C-6^{iv}), 143.7 (C-6^{vii}), 143.2 (C-7^{viii}), 142.4 (C-6'), 141.9 (C-6''), 140.7 (C-9a''' and 9a^{vi}), 138.6 (C-1^{vii}), 135.6 (C-7a''), 134.4 (C-7a'), 132.2 (C-5a^v and 5a^{viii}), 131.7 (C-1^{iv}), 131.4 (C-1), 129.9 (C-8a^{viii}), 125.0 (C-8a^v), 124.5 (C-6^{viii}), 124.4 (C-6^v), 122.7 (C-5^{iv}), 122.3 (C-5^{vii}), 122.1 (C-5^v), 121.9 (C-5^{viii}), 121.8 (C-8^{viii}), 121.8 (C-4^{iv}), 121.5 (C-8^v), 120.4 (C-4^{vii}), 119.8 (C-4'), 119.1 (C-4''), 119.0 (C-2), 119.0 (C-2^{vii}), 118.6 (C-6), 118.4 (C-5'), 118.2 (C-5''), 117.6 (C-2^{iv}), 116.8 (C-7''), 116.7 (C-7'), 111.4 (C-5), 107.1 (C-3), 23.8 ($CO\underline{CH_3}$); UV-Vis λ_{max} (MeOH) (Log ε): 272 (4.67), 348 (4.87), 437 (4.25), 483 (4.25), 555 (3.75) nm; IR (KBr) ν_{max}: 3285 (O-H and N-H), 3097 (ArC-H), 1654 (C=O), 1599 (C=N), 1512 (C=C), 1442 (N=N), 1269 (C-S), 1234 (C-O), 910-502 (Ar def C=N str thiazole) cm^{-1}; ms: (ESI^+) *m/z* (%) 1052 (4), 996 (3), 882 (3), 713 (3), 694 (3), 659 (3), 637 (7), 599 (13), 409 (16), 317 (26), 316 (81); Anal. Calcd. for $C_{50}H_{33}N_{25}O_{26}S_8$: C, 36.26; H, 2.01; N, 21.14; S, 15.48. Found: C, 36.24; H, 1.98; N, 21.17; S, 15.43. Rf = 0.53.

3,11-Dinitrobenzo[4,5]thiazolo[3,2-*c*]benzo[4,5]thiazolo[3,2-*e*][1,2,3,5]tetrazine-8,14-diium sulfate (**4c**). Compound **4c** was obtained in 41% yield as orange powder; m.p. 245 – 247 °C; ^{1}H-NMR (DMSO-d_6, 600 MHz): δ 8.95 (d, 1H, *J* 1.8 Hz, H-7), 8.69 (d, 1H, *J* 2.4 Hz, H-7'), 8.29 (s, 2H, NH), 8.25 (dd, 1H, *J* 2.8 and 8.8 Hz, H-5), 8.11 (dd, 1H, *J* 2.4 and 8.8 Hz, H-5'), 7.90 (d, 1H, *J* 8.8 Hz, H-4), 7.42 (d, 1H, *J* 8.8 Hz, H-4'); ^{13}C-NMR (DMSO-d_6, 150 MHz): δ 153.2 (C-2), 155.0 (C-3a), 121.0 (C-4), 122.5 (C-5 and C-5'), 144.0 (C-6), 119.3 (C-7), 132.6 (C-7a), 172.3 (C-2'), 158.7 (C-3a'), 117.3 (C-4'), 141.2 (C-6'), 118.3 (C-7'), 131.9 (C-7a'); **UV-Vis (MeOH)** λ_{max} (log *ε*): 260 (4.54), 285 (4.48), 352 (4.66), 393 (4.62), 421 (4.63), 450 (4.64), 472 (4.62); **IR (KBr)** υ_{max}/cm^{-1}: 3097 (C_{Ar}-H), 1556 (C=N), 1444 (N=N), 1336 (C_{Ar}-NO_2), 1120 (C-S), 1514 (C=C); ms: (ESI^+) *m/z* (%) 590 (5), 568 (3), 562 (10), 558 (15), 554 (10), 550 (17), 514 (35), 450 (76), 378 (10), 294 (13), 248 (34). Anal. Calcd. for: $C_{14}H_{18}N_6O_{14}S_3$: C, 28.48; H, 3.07; N, 14.23; S, 16.29. Found: C, 28.50; H, 3.1; N, 14.25; S, 16.32. Rf = 0.45.

1,2-Bis(6-nitrobenzothiazol-2-yl)diazene-1,2-diium sulfate (4c'). Compound **4c'** was obtained in 28% yield as red powder; m.p. 243 – 245 °C; ^{1}H-NMR (DMSO-d_6, 600 MHz): δ 8.69 (d, 2H, *J* 2.4 Hz, H-7 and H-7'), 8.24 (s, 2H, NH), 8.10 (dd, 2H, *J* 2.4 and 8.8 Hz, H-5 and H-5'), 7.42 (d, 1H, *J* 8.8 Hz, H-4 and H-4'); ^{13}C-NMR (DMSO-d_6, 150 MHz): δ 172.3 (C-2 and C-2'), 159.1 (C-3a and C-3a'), 117.3 (C-4 and C-4'), 122.5 (C-5 and C-5'), 141.2 (C-6 and C-6'), 118.2 (C-7 and C-7'), 132.1 (C-7a and C-7a'). **UV-Vis (MeOH)** λ_{max} (log *ε*): 269.7 (4.53), 279.6 (4.30), 351.3 (5.17); **IR (KBr)** υ_{max}/cm^{-1}: 3508 (N-H), 3068 (C_{Ar}-H), 1644 (C=N), 1568 (C=C), 1486 (N=N), 1282 (C_{Ar}-NO_2), 1120 (C-S); ms: (ESI^+) *m/z* (%) 484 (5), 452 (100), 456 (5), 466 (8), 438 (10), 428 (17). Anal. Calcd. for $C_{14}H_8N_6O_8S_3$: C, 34.71; H, 1.66; N, 17.35; S, 19.85 Found: C, 34.73; H, 1.70; N, 17.33; S, 19.88. Rf = 0.48.

Anticancer activity study

Chemicals

Dimethyl sulfoxide (DMSO) and (3-(4,5-dimethylthiazol-2-yl)-2,5-diphenyltetrazolium bromide) (MTT) were purchased from Sigma (St. Louis, Mo., USA). Fetal bovine serum and DMEM cell culture medium were provided by Highveld Biological, Johannesburg, South Africa. Trypsin-EDTA and penicillin were obtained from Virbac, South Africa.

Cell culture and maintenance

The effect of compounds on tumor cell proliferation was determined against three human cancer cell lines purchased from the American Type Culture Collection (ATCC), namely: A549 ATCC® CCL-185™ (Human Lung carcinoma); HeLa ATCC® CCL-2™ (Human cervical adenocarcinoma); MCF 7 ATCC ® HTB-22™ (Human breast adenocarcinoma); and one non-cancerous cell line Vero ATCC® CCL-81™ (Monkey Kidney). Cells were cultured in DMEM medium. All media used were supplemented with 10% fetal bovine serum (FBS), 100 IU/mL penicillin. The cell lines were maintained in DMEM under standard cell culture conditions at 37 ^{o}C and 5% CO_2 in a humidified environment.

MTT assay

The cytotoxicity of the compounds was assessed by the MTT reduction assay as previously described[36] with slight modifications. Cells were seeded at a density of 10^5 cells/mL (100 µL) in 96-well microtitre plates and incubated at 37 ^{o}C and 5% CO_2 in a humidified environment. After 24 h incubation, 100 µL of compounds at varying final concentrations prepared in DMEM were added to the wells containing cells. Doxorubicin was used as a positive control. A suitable blank control with equivalent concentrations of acetone was also included and the plates were further incubated for 48 h in a CO_2 incubator. Thereafter, the medium in each well was aspirated from the cells, which were then washed with PBS, and finally fresh DMEM (200 µL) was added to each well. Then, 30 µl of MTT (5 mg/mL in PBS) was added to each well and the plates were incubated at 37 °C for 4 h. The medium was aspirated from the wells and DMSO (50 µL) was added to solubilize the formed formazan crystals. The absorbance was measured on a BioTek Synergy microplate reader at 570 nm. The concentration causing 50% inhibition of cell growth (IC_{50}) was calculated from the concentration-inhibition response curve by regression analysis. The selectivity index (SI) values were calculated by dividing the IC_{50} values of the normal Vero cells by those of the cancer cells. Samples were tested in quadruplicate and each experiment was repeated thrice.

Acknowledgements

J. T is grateful to Gilbert Kirsch and Véronique Vaillant for running the NMR spectra. Additional financial supports for the work were obtained from the Cameroonian Ministry of Higher Education special research allocation. They authors are also grateful to the German Academic Exchange Service (DAAD) (grant N° 91691265) for SFE and DAAD (YaBiNaPA, project no. 57316173) for Bruno N. Lenta for the financial support granted to the Yaoundé-Bielefeld Graduate School of Natural Products with Antiparasite and Antibacterial Activities. JPD is grateful to DAAD for support through the Staff Exchange in Sub-Saharan Africa in the Phytomedicine Programme. The University of Pretoria is thanked for postdoctoral support to IMF.

Supplementary Material

Electronic Supplementary Information (ESI) available: copies of the UV, IR, MS, ^{1}H and ^{13}C NMR spectra for all new compounds.

References

1. Nagai, H.; Kim, Y. H. *J. Thorac. Dis.* **2017**, 9, 448-451. https://doi.org/10.21037/jtd.2017.02.75
2. Khan, F. A.; Akhtar, S. S.; Sheikh, M. K. *Malays. J. Med. Sci.* **2005**, 12, 3-5.
3. Nie, Z.; Kumacheva, E. *Nat. Mater.* **2008**, *7*, 277-290. https://doi.org/10.1038/nmat2109
4. Obadia, M. M.; Drockenmuller, E. *Chem. Commun.* **2016**, *52,* 2433–2450. https://doi.org/10.1039/C5CC09861K
5. Sletten, E. M.; Bertozzi, C. R. *Angew. Chem. Int. Ed.* **2009**, *48*, 6974-6998. https://doi.org/10.1002/anie.200900942
6. Wang, T.; Zheng, C.; Yang, J.; Zhang, X.; Gong, X.; Xia, M. *J. Mol. Model.* **2014**, *20*, 2261–2271. https://doi.org/10.1007/s00894-014-2261-1
7. Saracoglu, N. *Tetrahedron* **2007**, *63*, 4199–4235. https://doi.org/10.1016/j.tet.2007.02.051
8. Sinditskii, V. P.; Egorshev, V. Y.; Rudakov, G. F.; Filatov, S. A.; Burzhava, A. V. Springer International Publishing: Cham, Switzerland, **2017**; 45, 89–125. https://doi.org/10.1007/978-3-319-27748-6_3
9. Devaraj, N. K.; Upadhyay, R.; Haun, J. B.; Hilderbrand, S. A.; Weissleder, R. *Angew. Chem. Int. Ed.* **2009**, *48(38)*, 7013-7016. https://doi.org/10.1002/anie.200903233
10. Devaraj, N. K.; Weissleder, R. *Acc. Chem. Res.* **2011**, *44*, 816–827. https://doi.org/10.1021/ar200037t
11. Liu, D. S.; Tangpeerachaikul, A.; Selvaraj, R.; Taylor, M. T.; Fox, J. M.; Ting, A. Y. *J. Am. Chem. Soc.* **2012**, *134*, 792–795. https://doi.org/10.1021/ja209325n
12. Seitchik, J. L.; Peeler, J. C.; Taylor, M. T.; Blackman, M. L.; Rhoads, T. W.; Cooley, R. B.; Refakis, C.; Fox, J. M.; Mehl, R. A. *J. Am. Chem. Soc.* **2012,** *134*, 2898-2901. https://doi.org/10.1021/ja2109745
13. Koo, H.; Choi, M.; Kim, E.; Hahn, S. K.; Weissleder, R.; Yun, S. H. *Small.* **2015**, *11*, 6458-6466. https://doi.org/10.1002/smll.201502972
14. Liu, S., Dicker, K. T., Jia, X. *Chem. Commun*. **2015**, *51*, 5218–5237. https://doi.org/10.1039/C4CC09568E
15. Carthew, J.; Frith, J. E.; Forsythe, J. S.; Truong, V. X. *J. Mater. Chem. B* **2018**, *6*, 1394-1401. https://doi.org/10.1039/C7TB02764H
16. Jain, S.; Neumann, K.; Zhang, Y.; Geng, J.; Bradley, M. *Macromolecules* **2016**, *49*, 5438–5443. https://doi.org/10.1021/acs.macromol.6b00867

17. Discekici, E. H.; St Amant, A. H.; Nguyen, S. N.; Lee, I. H.; Hawker, C. J.; Read de Alaniz, J. *J. Am. Chem. Soc.* **2018**, *140*, 5009-5013. https://doi.org/10.1021/jacs.8b01544
18. Alge, D. L.; Azagarsamy, M. A.; Donohue, D. F.; Anseth, K. S. *Biomacromolecules* **2013**, *14*, 949-953. https://doi.org/10.1021/bm4000508
19. Roling, O.; Mardyukov, A.; Lamping, S.; Vonhoren, B.; Rinnen, S.; Arlinghaus, H. F.; Studer, A.; Ravoo, B. J. *Org. Biomol. Chem.* **2014**, *12*, 7828. https://doi.org/10.1039/C4OB01379D
20. Sun, H.; Chen, G. Y. J.; Yao, S. Q. *Chem. Biol.* **2013**, *20*, 685-699. https://doi.org/10.1016/j.chembiol.2013.04.009
21. Blackman, M. L.; Royzen, M.; Fox, J. M. *J. Am. Chem. Soc.* **2008**, *130*, 13518-13519. https://doi.org/10.1021/ja8053805
22. Royzen, M.; Yap, G. P. A.; Fox, J. M. *J. Am. Chem. Soc.* **2008**, *130*, 3760-3761. https://doi.org/10.1021/ja8001919
23. Yang, M. R. K. J.; Li, W.; Sahu, S.; Devaraj N. K. *Angew. Chem. Int. Ed.* **2012**, *51*, 1-5. https://doi.org/10.1002/anie.201201117
24. Wahe, H.; Mbafor, T. J.; Nkengfack, A. E.; Fomum, Z. T.; Cherkasov, R. A.; Sterner, O.; Doepp, D. *Arkivoc* **2003**, (xv), 107-114. https://doi.org/10.3998/ark.5550190.0004.f12
25. Ambartsumova, R. F.; Kosmacheva, L. P. *Chem. Heterocycl. Compd.* **1991**, *27,* 547–551. https://doi.org/10.1007/BF00474005
26. Wiley R. H.; Jarboe Jr C. H.; Hayes, E. N. *J. Org. Chem*., **1957**, 835-836. https://doi.org/10.1021/jo01358a609
27. Tsemeugne, J.; Nangmo, P. K.; Mkounga, P.; Tamokou, J. D. D.; Kengne, I. C.; Edwards, G.; Sopbué, E. F.; Nkengfack, A. E. Heterocycl. Commun**. 2021**, *27*, 79-89.
28. Mason, S. F. *J. Chem. Soc.* **1959**, 1240-1246. https://doi.org/10.1039/JR9590001240
29. Hochstra, Rm; King, D. S. *Chem. Phys.* **1974**, *5*, 439-447. https://doi.org/10.1016/0301-0104(74)85045-7
30. Syarifah, S. M. M.; Nurhanan, MY; Haffiz, J. M.; Ilham, A. M.; Getha, K.; Asiah, O; Norhayati, I.; Sahira, H. L.; Suryani, S. A. *J. Trop. Forest Sci.* **2011**, *23*, 89-96.
31. Irfan, A.; Batool, F.; Zahra, N. S.; Islam, A.; Osman, S. M.; Nocentini, A.; Alissa, S. A.; Supuran, C. T. *J. Enzyme Inhib. Med. Chem.* **2020**, *35*, 265-279. https://doi.org/10.1080/14756366.2019.1698036
32. Fu, D. J.; Liu, S. M.; Li, F. H.; Yang, J. J.; Li, J. *J. Enzyme Inhib. Med. Chem*. **2020,** *35*, 1050-1059. https://doi.org/10.1080/14756366.2020.1753721
33. Brahemi, G.; Kona, F. R.; Fiasella, A.; Buac, D.; Soukupová, J.; Brancale, A.; Burger, A. M.; Westwell, A. D. *J. Med. Chem.* **2010**, *53*, 2757–2765. https://doi.org/10.1021/jm901757t
34. Hu, W. X.; Rao, G. W.; Sun, Y. Q. *Bioorg. Med. Chem. Lett.* **2004,** *14*, 1177-1181. https://doi.org/10.1016/j.bmcl.2003.12.056
35. Cañete-Molina, Á.; Espinosa-Bustos, C.; González-Castro, M.; Faúndez, M.; Mella, J.; Tapia, R. A.; Cabrera, A. R.; Brito, I.; Aguirre, A.; Salas, C. O. *Arab. J. Chem.* **2019**, *12*, 1092-1107. https://doi.org/10.1016/j.arabjc.2017.04.002

36. Dzoyem, J. P.; McGaw, L. J.; Eloff, J. N.; *BMC Complement Altern. Med.* **2014**, 14:147. https://doi.org/10.1186/1472-6882-14-147